

# Photo-Induced Thiolate Catalytic Activation of Inert C<sub>aryl</sub>-Hetero Bonds for Radical Borylation

Shun Wang, Hua Wang, and Burkhard König\*

Institute of Organic Chemistry, Faculty of Chemistry and Pharmacy, University of Regensburg, D-93040  
Regensburg, Germany

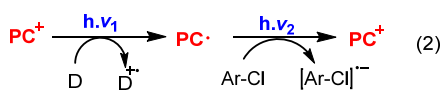
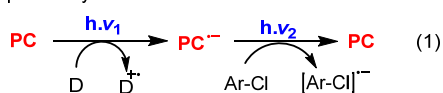
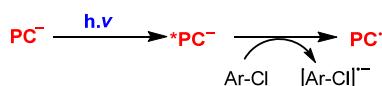
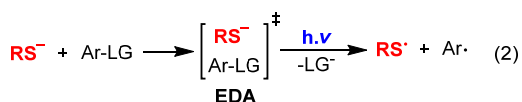
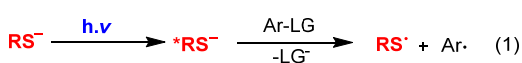
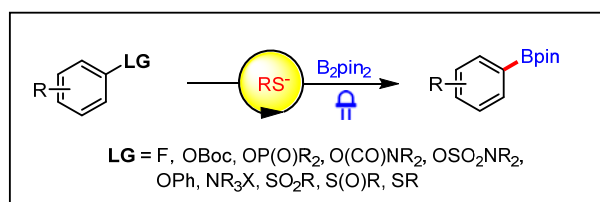
\*Correspondence: [burkhard.koenig@ur.de](mailto:burkhard.koenig@ur.de)

## Abstract

Substantial effort is currently devoted to obtain high redox energy photoredox catalysts. Yet, it remains challenging to apply the currently established methods to the activation of bonds with high bond dissociation energy and to substrates with high reduction potentials. Herein, we introduce a novel photocatalytic strategy for the activation of inert substituted arenes for aryl borylation by using thiolate as a catalyst. This catalytic system exhibits strong reducing ability and engages non-activated C<sub>aryl</sub>-F, C<sub>aryl</sub>-O, C<sub>aryl</sub>-N and C<sub>aryl</sub>-S bonds in productive radical borylation reactions, thus expanding the available aryl radical precursor scope. Despite its high reducing power, this demonstrates broad substrate scope and functional group tolerance. The spectroscopic investigations, NMR analysis, and control experiments suggest the formation of a charge-transfer complex as the key step to activate the substrates.

## Introduction

Photoredox catalysis has emerged as a powerful technique in organic synthesis over the past decade through converting the energy of photons into redox energy for chemical processes. This empowers organic chemists to realize a number of unprecedented chemical transformations under mild conditions for organic synthesis.<sup>1-6</sup> However, the range of attainable redox potentials in typical photocatalysis system is governed by the energy of the absorbed photon. Intersystem crossing and non-radiative pathways diminished this energy inevitably.<sup>7</sup> Thus, it is challenging to activate high redox energy demanding substrates by visible-light-irradiation. For instance, reductive transformations, particularly those that require highly reducing power, remain an underdeveloped field. To this end, considerable efforts have been devoted towards the development of new photocatalytic systems with high reduction ability over past few years. To overcome the thermodynamic limits, several approaches to accumulate the energy of two or more photons enhancing the reducing power of a photocatalyst have been established.<sup>7-10</sup> We have reported a consecutive photoinduced electron transfer (conPET) utilizing two photons via excitation of photogenerated radical anions (**Scheme 1A**, equation 1).<sup>11-13</sup> Likewise, photoexcitation of electrochemically generated radical anions was shown to be capable of generating high reduction power.<sup>14, 15</sup> Nicewicz et al. showed that the acridine radical ACR• could act as an extremely potent photoreductant upon excitation with light (**Scheme 1A**, equation 2).<sup>16</sup> Moreover, direct photoexcitation of an organo-anionic species has been demonstrated to provide exciting opportunities to access highly reducing reactive intermediates (**Scheme 1B**).<sup>10, 17</sup>

**A Two photon system****B Excitation of anionic species****C Possible photo-induced activation of substituted arenes by using thiolate as a catalyst (Reaction design)****D This work:** photocatalytic borylation of inert C-F, C-O, C-N & C-S bonds**Scheme 1.** Photocatalytic strategies to access high reduction power for SET activation of substituted arenes

Arylboronates are recognized as essential building blocks in organic synthesis, material science, and drug discovery.<sup>18-19</sup> Transition-metal-catalyzed Miyaura borylation of aryl halides has been developed as one of the most efficient method for synthesizing arylboron reagents.<sup>20, 21</sup> In recent years, photocatalytic borylation has attracted considerable research interest and opened a new avenue to access arylboronates.<sup>22-25</sup> A number of photo-induced systems were developed that allow for the borylation of aryl-X bonds from a wide range of substrates such as aryldiazonium salts,<sup>26-28</sup> aryl ammonium salt ammonium,<sup>29, 30</sup> aryl (pseudo) halides,<sup>15, 29-39</sup> and carboxylic acids.<sup>40</sup> However, most established photo-induced borylation methods are limited to substrates with labile aryl-hetero bonds or low reduction potentials. Thus, it remains highly challenging to apply the current methods to the borylation of inert bonds such as unactivated C<sub>aryl</sub>-F, C<sub>aryl</sub>-O, C<sub>aryl</sub>-N and C<sub>aryl</sub>-S bonds owing to their high bond dissociation energy and high reduction potentials of substrates. The development of a strategy for the borylation of these bonds would not only greatly widen the available substrate types to access arylboronates but also might represent a significant step towards utilizing unreactive bonds as functional groups in cross-coupling reactions.

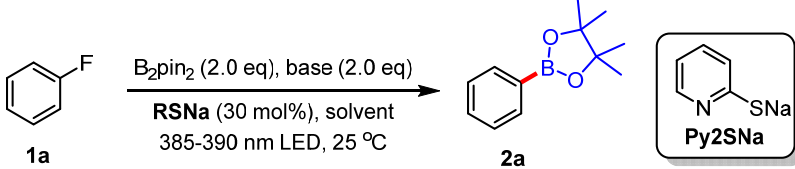
Continuing our research interest in exploring the reducing ability of anionic species in photoredox catalysis,<sup>41, 42</sup> we wondered whether we could generate aryl radicals from inert bonds (C<sub>aryl</sub>-F, C<sub>aryl</sub>-O, C<sub>aryl</sub>-N and C<sub>aryl</sub>-S bonds) for borylation by using a sulfur-centered anion (*e.g.*, thiolate) as a

photocatalyst. The proposed catalytic system was inspired by our previous finding wherein thiolate could efficiently shuttle electrons from the boronate radical anion, a species that is produced in radical borylation processes, to the photocatalytic system.<sup>43</sup> It was therefore hypothesized that using thiolate direct as a photocatalyst might offer an exciting opportunity for the activation of inert C<sub>aryl</sub>-X bonds to generate aryl radicals. In the anticipated activation of substituted arenes by thiolate photocatalysis, two possible reaction modes might be involved as shown in **Scheme 1C**: (1) direct interaction of substituted arenes with the excited state of thiolate. (2) formation of a charge transfer complex between thiolate catalyst and substituted arenes.<sup>44-50</sup> We report herein the successful application of thiolate catalysis for the photoinduced borylation of substituted arenes through the cleavage of non-activated C(sp<sup>2</sup>)-F, C(sp<sup>2</sup>)-O, C(sp<sup>2</sup>)-N and C(sp<sup>2</sup>)-S bonds (**Scheme 1D**).

## Results and discussion

We commenced the study by evaluating the defluoroborylation reaction of fluorobenzene (**1a**,  $E_{\text{red}} = -3.34$  V vs SCE in DMF) with B<sub>2</sub>pin<sub>2</sub> (bis(catecholato)diboron). Owing to the high bond dissociation energy of Ar-F bonds (e.g. BDE of Ph-F bond is 526 kJ·mol<sup>-1</sup>), only few examples are available for the borylation of unactivated aryl fluoride under transition-metal-free conditions at present.<sup>29, 35, 51</sup> To our delight, the desired borylated product **2a** was obtained in 33% yield at room temperature by irradiation with a 385-390 nm LED lamp using CsF as a base and sodium 3-methyl-phenyl thiolate (30% mol) as the catalyst (Table 1, entry 1). Studies with other thiolates revealed that Py2SNa (pyridine-2-thiolate) is the optimal catalyst yielding the product in 56% yield (entries 2-4). It is worth mentioning that CySNa (sodium cyclohexanethiolate) and 1-AdSNa (Sodium 1-Adamantanethiolate) showed comparably good catalytic performances affording the product while pyridine as a catalyst did not give the product (entry 5), thus indicating that in our reaction the reactivity stems from the thiolate under photocatalytic conditions. Changing the solvent from MeCN to DMSO or THF gave either a poor yield or trace amount of the product (entry 6 and 7). To further increase the yield, a variety of bases were examined. Tetramethylammonium fluoride (TMAF) turned out to be the optimal base, resulting in the formation of **2a** in 74% yield, the increase of reactivity likely attributed to its superior solubility in MeCN (entry 8). Using other bases such as KF, Cs<sub>2</sub>CO<sub>3</sub> and CsOAc failed to improve the yield (entries 9-11). In the absence of base, the reaction afforded **2a** in only 13% yield (entry 12). To our delight, the yield was further improved to 81% when slight excess amounts of B<sub>2</sub>pin<sub>2</sub> and TMAF were employed (entry 13). Control experiments showed that both thiolate catalyst Py2SNa and light irradiation (385-390 nm) were essential for this reaction (entries 14-16).

**Table 1. Evaluation of Reaction Conditions for the Borylation of Fluorobenzene with B<sub>2</sub>pin<sub>2</sub>**



Entry	Base	Catalyst	Solvent	Yield <sup>a</sup>
1	CsF	3-Me-PhSNa	MeCN	33%
2	CsF	CySNa	MeCN	48%
3	CsF	1-AdSNa	MeCN	40%
4	CsF	Py2SNa	MeCN	56%

5	CsF	pyridine	MeCN	n.d.
6	CsF	Py2SNa	DMSO	24%
7	CsF	Py2SNa	THF	trace
8	TMAF	Py2SNa	MeCN	74%
9	KF	Py2SNa	MeCN	19%
10	Cs <sub>2</sub> CO <sub>3</sub>	Py2SNa	MeCN	33%
11	CsOAc	Py2SNa	MeCN	27%
12	-	Py2SNa	MeCN	13%
Entry	Change from entry 8		Yield	
13	B <sub>2</sub> pin <sub>2</sub> (3.0 eq.), TMAF (3.0 eq.)		81% (78%) <sup>b</sup>	
14	455 nm LED		n.d.	
15	in the dark		trace	
16	no Py2SNa		10%	

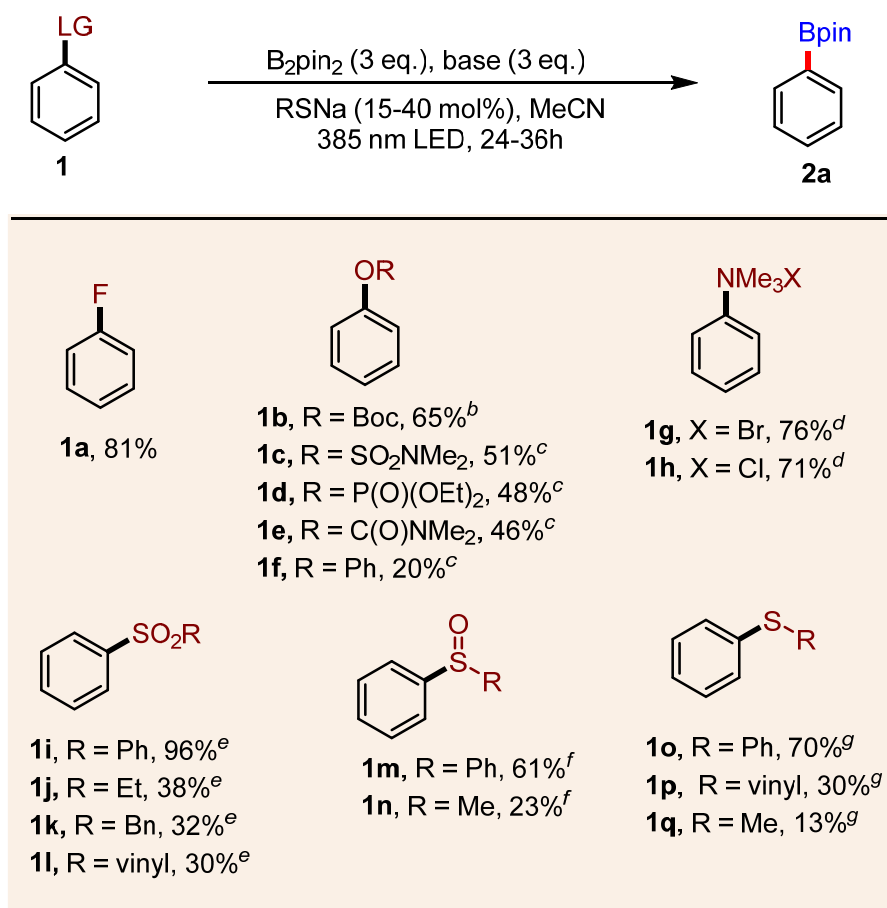
Reaction conditions: **1a** (0.2 mmol), B<sub>2</sub>pin<sub>2</sub> (0.4 mmol), base (0.4 mmol), catalyst (30 mol%), and in 2 mL of solvent, irradiation with a 385-390 nm LED (3.8 W) at 25 °C for 24 h under N<sub>2</sub> atmosphere. n.d. = not detected. TMAF= tetramethylammonium fluoride; B<sub>2</sub>pin<sub>2</sub> = bis(pinacolato)diboron; CySNa = sodium cyclohexanethiolate; 1-AdSNa = Sodium 1-Adamantanethiolate; Py2SNa = pyridine-2-thiolate; <sup>a</sup>Yields were determined by GC-FID analysis of the crude reaction mixture using dodecane as an internal standard. <sup>b</sup>Isolated yield.

Encouraged by these results, we next turned our attention to test the feasibility of this catalytic system with arene substrates bearing different leaving groups (Table 2). We first focused on the borylation of C-O bonds of phenol derivatives considering that phenols have emerged as versatile and cost-efficient alternatives to aryl halides.<sup>24, 52, 53</sup> It is worth mentioning that, unlike the use of reactive aryl sulfonates such as aryl triflates, mesylates or tosylates, few methods are known for catalytic radical borylation of less or even non-activated aryl esters as coupling partners via C-O bond-cleavage.<sup>24, 30, 38</sup> In particular, using a slightly modified reaction condition (see the SI for details), O-Boc-protected phenol **1b** could be borylated efficiently to give product **2a** in 65% yield. To the best of our knowledge, this is the first example of transition metal-free borylation of aryl carbonates via C-O bond cleavage. Furthermore, we found that the reaction system was also feasible for sulfamate **1c**, phosphate **1d** and carbamate **1e**. Interestingly, even C-O bonds of diphenylether showed a certain degree of reactivity in the reaction. Arylammonium salts **1g** and **1h** were also viable for this transformation leading to C-N borylated products in 76% and 71% yield, respectively.

Given that organosulfur compounds are widely present in natural products, drugs and proteins, our protocol was briefly examined as a viable route for the C-S bond borylation of sulfur-containing molecules, which allows modification of their structures.<sup>54-56</sup> Indeed, the C-S bond of diphenyl sulfone **1i** could be borylated efficiently to give product **2a** in excellent yield. When alkyl phenyl sulfones (**1j** and **1k**) and vinyl phenyl sulfone **1l** were used, the borylation occurred selectively at the phenyl-SO<sub>2</sub> bonds to give aryl boronic ester product **2a**, while the alkyl boronic esters were merely observed in trace amounts. The reactivity is in contrast to Nambo and Crudden's observation, wherein the borylation of alkyl phenyl sulfones occurred predominately to afford alkyl boronic esters in a pyridine catalytic system.<sup>57</sup> Other than sulfones, our strategy permitted the use of diphenyl sulfoxide and methyl phenyl sulfoxides (**1m** and **1n**) as the phenyl radical precursors for borylation, albeit the reaction in the latter case proceeds with lower efficiency. Subsequently, we were glad to

find that this methodology was applicable to convert aryl sulfides to aryl boronic esters through C-S cleavage. Specifically, diphenyl sulfide reacted smoothly to give **2a** in a 70% yield, while vinyl phenyl sulfide demonstrated diminished reactivity. Attempts to borylate thioanisole **1q** was unsuccessful, giving the target product **2a** in 13% yield. These results are particularly noteworthy considering the fact that thiolate anions are rarely used as leaving groups in radical arylation reactions and sulfides possess more negative reduction potentials, which are caused by the electron-donating property of SR groups.<sup>8, 58</sup>

**Table 2. Leaving group scope for photo-induced *ipso*-borylation of substituted arenes<sup>a</sup>**



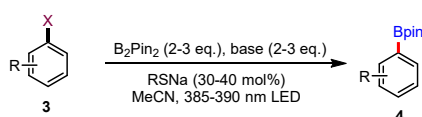
<sup>a</sup>Reaction condition: **1** (0.2 mmol), B<sub>2</sub>pin<sub>2</sub> (3.0 eq.), base (3.0 eq.), Py<sub>2</sub>SNa (15-40 %mol), in 2 mL of MeCN, irradiation with a 385-390 nm LED (3.8 W) at 25 °C for 24 h under N<sub>2</sub> atmosphere. Yields were determined by GC-FID using n-dodecane as an internal standard. <sup>b</sup>CsF (3.0 eq.), Py<sub>2</sub>SNa (40 mol%), 36 h. <sup>c</sup>TMAF (3.0 eq.), MeCN (1.5 mL), 36 h. <sup>d</sup>KOAc (3.0 eq.), Py<sub>2</sub>SNa (15 mol%), MeCN (1.5 mL). <sup>e</sup>CsF (3.0 eq.), 1-AdSNa (30 mol%). <sup>f</sup>B<sub>2</sub>pin<sub>2</sub> (2.0 eq.), CsF (2.0 eq.), CySNa (30 mol%). <sup>g</sup>B<sub>2</sub>pin<sub>2</sub> (2.0 eq.), CsF (2.0 eq.), 1-AdSNa (30 mol%).

After surveying the scope of phenyl radical precursors, we next sought to study the preparative scope of our reaction utilizing substituted aryl fluorides, O-Boc protected phenols as well as organosulfur compounds. We were pleased to see a wide variety of aryl fluorides bearing *para*-(**3b**–**3o**), *ortho*-(**3p** and **3q**) and *meta*-(**3r**–**3u**) substituents reacting smoothly to afford the corresponding boronic esters. A broad range of substituents at the *para*-position, including strongly electron-donating groups such as –OMe (**3d**), piperidinyl (**3i**), –NH<sub>2</sub> (**3j**), as well as electron-neutral ethyl (**3b**), benzyl (**3c**) and boronic ester (**3l**)

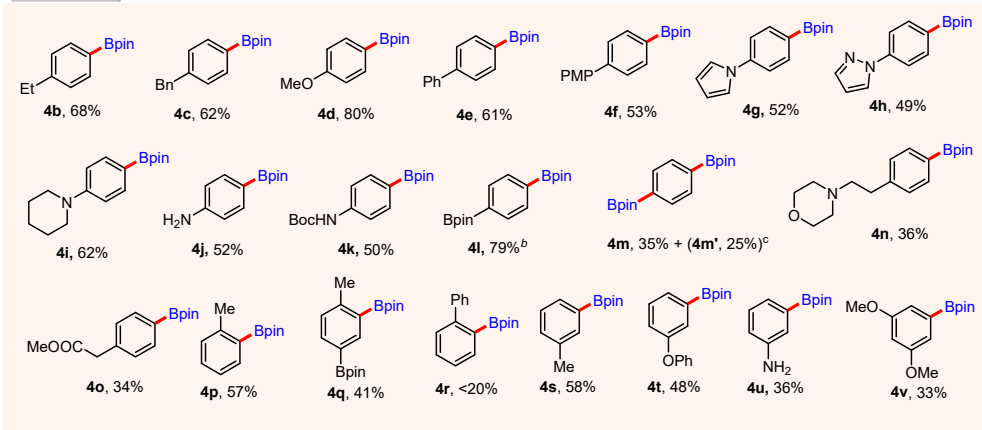
groups, were all tolerated and provided the desired products in good yields. The presence of acidic protons in amine (**3j**) and amide (**3f**) did not interfere with the reaction. Aromatic substituents, such as aryl (**3e** and **3f**), pyrrole (**3g**) and pyrazole (**3h**) were compatible with the reaction conditions. Substrates bearing functional groups such as morpholine and ester on the alkyl chains also reacted smoothly to give the products (**3n** and **3o**). *Ortho*-methyl substituted aryl fluorides (**3p** and **3q**) reacted smoothly to provide the products in 57% and 41% yield respectively, whereas more sterically hindered phenyl groups at the *ortho*-position inhibited the reactivity with the hydrodefluorination product being detected as the major byproduct. *Meta*-substituted aryl fluorides bearing various functional groups such as phenoxy and amine showed good reactivity in the reaction conditions. Notably, aryl fluorides bearing two methoxy groups also reacted to furnish the corresponding product (**4v**) in 33% yield, highlighting the high reactivity of the catalytic system.

Prompted by these results, we next proceeded to explore the scope of the *ipso*-borylation of Ar–OBoc and Ar–S bonds. We were delighted to find that many synthetically useful functional groups including alkyl (**4w** and **4ab**), phenyl (**4e**), phenoxy (**4x**), amide (**4k**) and alkoxy (**4aa** and **4ac**) substituents on the phenyl ring of Boc-protected phenols could be tolerated, providing the products in moderate yields. These results are noteworthy considering that the electron rich Boc-protected phenols should possess very negative reduction potentials. Moreover, amide **4y** and ester **4z** functionalities on the alkyl chain of the phenolic compounds remained untouched in the reaction conditions. The synthetic utility of this chemistry was further demonstrated by the successful borylation of a  $\delta$ -tocopherol derivative, affording the product **4ad** in 65% yield. Finally, the borylation of diarylsulfones bearing methyl, methoxy and phenyl groups were fruitful in giving product yields of the isolated boronic esters (**4d**, **4e** and **4w**) ranging from 64% to 72%. Besides, methoxy-substituted diaryl sulfoxide and sulfide were also suitable substrates for borylation.

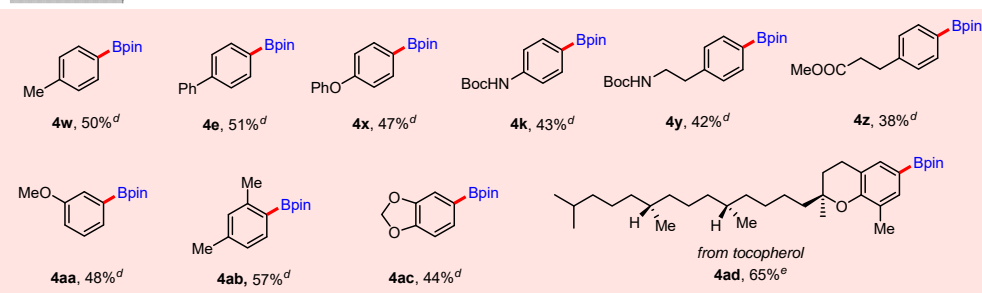
**Table 3. Substrate Scope for Photo-induced *Ips*o-Borylation<sup>d</sup>**



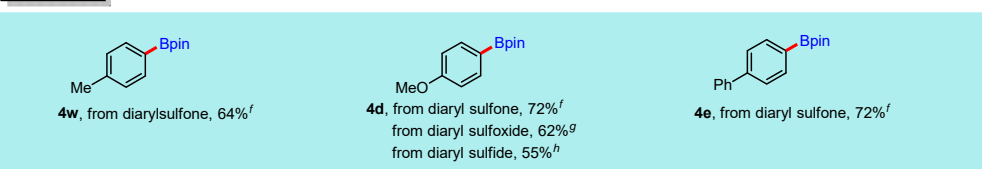
**C-F bonds**



**C-O bonds  
(X = OBoc)**



**C-S bonds**



<sup>a</sup>Reaction conditions: **3** (0.2 mmol), B<sub>2</sub>pin<sub>2</sub> (3.0 eq.), TMAF (3.0 eq.), Py<sub>2</sub>SNa (30 %mol), in 2 mL of MeCN, irradiation with a 385-390 nm LED (3.8 W) at 25 °C for 24 h under N<sub>2</sub> atmosphere, and isolated yields were shown.

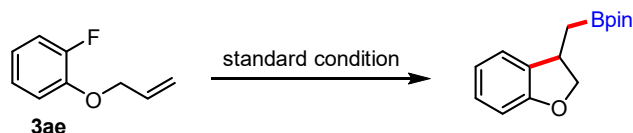
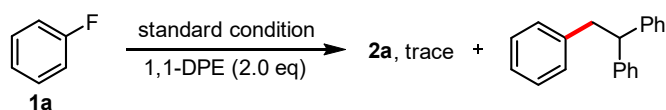
<sup>b</sup>CsF (3.0 eq.), B<sub>2</sub>pin<sub>2</sub> (3.0 eq.). <sup>c</sup>TMAF (4.0 eq.), B<sub>2</sub>pin<sub>2</sub> (4.0 eq.), **4m'**: mono-borylation product. <sup>d</sup>CsF (3.0 eq.), Py<sub>2</sub>SNa (40 mol%), 36 h. <sup>e</sup>X = OSO<sub>2</sub>NMe<sub>2</sub>, Py<sub>2</sub>SNa (40 % mol), MeCN (1.5 mL). <sup>f</sup>CsF (3.0 eq.), 1-AdSNa (30 mol %). <sup>g</sup>CsF (2.0 eq.), B<sub>2</sub>pin<sub>2</sub> (2.0 eq.), CySNa (30 mol%). <sup>h</sup>CsF (2.0 eq.), B<sub>2</sub>pin<sub>2</sub> (2.0 eq.), 1-AdSNa (30 mol%).

### Mechanistic studies

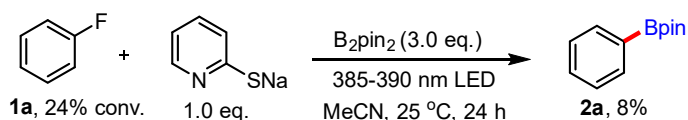
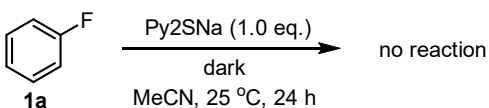
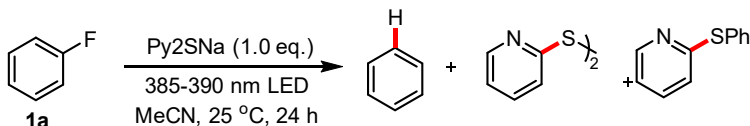
To obtain mechanistic insights into the reaction mechanism, a number of experimental studies were carried out. At the outset, the effect of radical scavengers on the current borylation system was examined (**Scheme S1** and **Figure 1A**). The presence of 1,1-DPE (1,1-diphenylethylene) inhibited the reaction completely, and the corresponding trapping adducts were formed in 5% yield. When aryl fluoride **3ae** with an *ortho*-allyloxy side chain was subjected to the standard conditions, cyclic alkylboronate **4ae** derived from a radical addition-borylation sequence was detected in 13% yield. These results collectively suggest the intermediacy of the phenyl radical in the reaction. To elucidate the radical generation process, further control experiments were conducted. Under light irradiation (385 nm), fluorobenzene **1a** reacted with Py2SNa to give benzene, disulfide and sulfide albeit in low conversion (16%), whereas no reaction could be observed in the dark (**Figure 1B**, equation 1-2). These results imply that phenyl radical and sulfur radical could be generated through direct photo-induced electron transfer between the thiolate and fluorobenzene with low efficiency.

Next, we performed UV-vis spectroscopic measurements of reaction components to explore the electron transfer process between Py2SNa and **1a**. It turned out that absorption spectra of B<sub>2</sub>pin<sub>2</sub>, substrate **1a**, and TMAF showed bands exclusively in the UV region (<300 nm) (**Figure S5**). However, Py2SNa was observed to absorb light at 390 nm, addition of B<sub>2</sub>pin<sub>2</sub> (1.0 eq.) led to a clear redshift by ~50 nm in absorption. A further significant redshift appeared when TMAF and **1a** were added to the mixture of Py2SNa and B<sub>2</sub>pin<sub>2</sub>, while this signal change was not observed in the absence of TMAF (**Figure 1C**). Fluorescence measurements showed that the emission of Py2SNa was not quenched by adding substrates **1a** and B<sub>2</sub>pin<sub>2</sub>. On the contrary, the fluorescence intensity of Py2SNa was markedly enhanced by the addition of B<sub>2</sub>pin<sub>2</sub>, **1a** and TMAF, excluding the interaction of the substrate with the excited state of thiolate (**Figure S6**). These results support the formation of a charge-transfer complex in the reaction process.<sup>59, 60</sup>

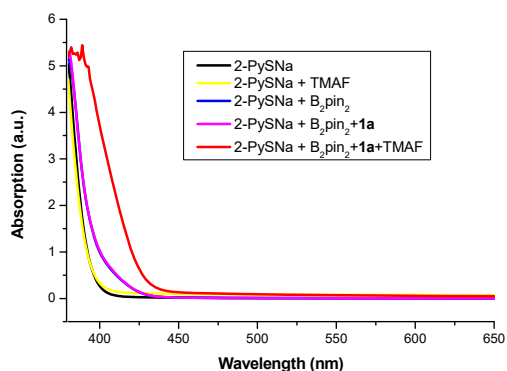
### (A) Radical inhibition experiments



### (B) Control experiments



### (C) UV-vis measurements



### (D) $^{19}\text{F}$ NMR experiments

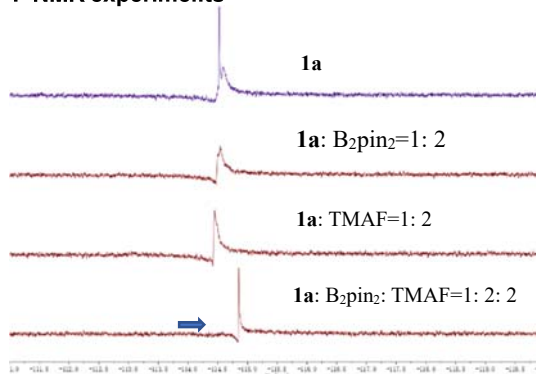
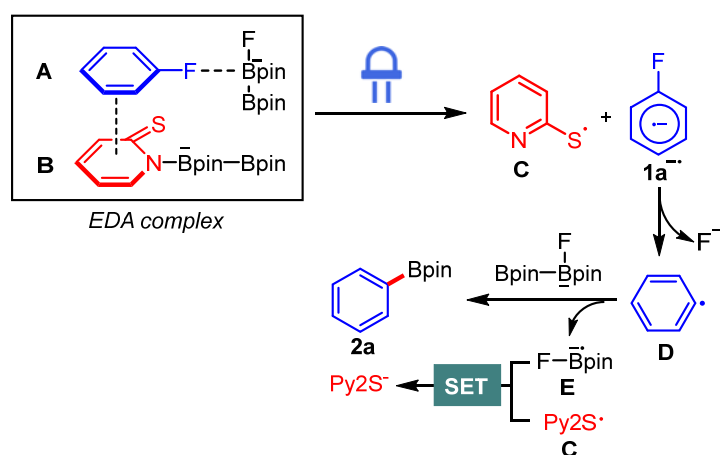


**Figure 1.** Mechanistic studies. (A) Radical trapping experiments. (B) Control experiments to elucidate the mechanism. (C) UV-vis spectra of reaction components. (D)  $^{19}\text{F}$  NMR spectra of **1a** in the presence of  $\text{B}_2\text{pin}_2$ , and/or TMAF

Moreover, we were intrigued by the redshift in the UV-vis spectrum of  $\text{Py}_2\text{SNa}$  by adding  $\text{B}_2\text{pin}_2$ .  $^{11}\text{B}$  NMR spectroscopic analysis revealed that a new peak with a chemical shift of 8.8 ppm appeared upon mixing  $\text{B}_2\text{pin}_2$  with  $\text{Py}_2\text{SNa}$ , suggesting the formation of an anionic diboron species (**Figure S7**). Meanwhile, it was observed that, both  $^1\text{H}$  NMR and  $^{13}\text{C}$  NMR signals of  $\text{Py}_2\text{SNa}$  were shifted with 1.0 equivalent of  $\text{B}_2\text{pin}_2$  added, confirming the formation of a new boryl species. Considering the ease with which diboronate esters can react with pyridine type bases to form the corresponding Lewis base adducts,<sup>40, 61-63</sup> it was postulated therefore that a Lewis acid–base adduct formed between  $\text{Py}_2\text{S}^-$  and

B<sub>2</sub>pin<sub>2</sub> was responsible for the observed redshift.

Further control experiments demonstrated that in the absence of fluoride a low conversion of **1a** (24%) and only 8% borylation product **2a** were observed (Figure 1B, equation 3). We thus suspect that it is very likely that the activation of fluorobenzene by the co-existence of fluoride and B<sub>2</sub>pin<sub>2</sub> could facilitate the SET between thiolate and **1a**. Subsequently, we observed a C-F chemical shift moving upfield from -114.51 to -114.84 ppm after mixing **1a** with 2.0 equivalents of B<sub>2</sub>pin<sub>2</sub> and TMAF, while the C-F chemical shift was not affected by B<sub>2</sub>pin<sub>2</sub> or TMAF separately (Figure 1D and S11). Cyclic voltammetry (CV) analysis demonstrated that the reduction potential of fluorobenzene was decreased considerably by adding TMAF and B<sub>2</sub>pin<sub>2</sub> (Figure S4). On the other hand, we observed the formation of a sp<sup>2</sup>-sp<sup>3</sup> fluoride diborane adduct between TMAF and B<sub>2</sub>pin<sub>2</sub> by <sup>19</sup>F NMR measurements (Figure S10).<sup>37, 64, 65</sup> We thus propose that an *in-situ* generated nucleophilic boryl anion species [B<sub>2</sub>pin<sub>2</sub>F]<sup>-</sup> could activate fluorobenzene **1a**, facilitating the single electron transfer and subsequent fluoride leaving process.



**Scheme 2.** Mechanistic proposal

Based on the aforementioned results and mechanistic pathways previously reported in literature, we propose the mechanism depicted in Scheme 2. The reaction sequence is initiated by the formation of an EDA complex between boryl anion-activated fluorobenzene **A** and Py<sub>2</sub>SNa/B<sub>2</sub>pin<sub>2</sub> adduct **B**. Upon photoexcitation of the EDA complex, an inner-sphere electron transfer occurs to afford thiyl radical **C** and radical anion of **1a**.<sup>66</sup> The resulting radical anion undergoes cleavage of the C-F bond to form the phenyl radical, which then reacts with a sp<sup>3</sup>-sp<sup>2</sup> diboron species [FB<sub>2</sub>pin<sub>2</sub>]<sup>-</sup> to give the desired borylation product **2a** and boryl radical anion **E**. Finally, the thiyl radical **C** was reduced by boryl radical anion **E** to regenerate thiolate closing the catalytic cycle.

## Conclusion

In summary, we have developed a new photocatalytic strategy for the *ipso*-borylation of substituted arenes using thiolate as a catalyst. This strategy realized the borylation of a very broad range of inert C-X bonds including non-activated C-F, C-O bonds of phenol derivatives (carbonate, sulfamate, phosphate and carbamate), C-N bond of ammonium salts and C-S bonds (sulfone, sulfoxide and sulfide) with very negative reduction potentials, which are challenging using existing photoredox activation. In this manner, this system allows the utilization of a range of unconventional leaving groups for radical borylation reactions, thus expanding available substrate types to access arylboronates. Despite the generated high

reducing power, this reaction displays broad functional group tolerance, and furnishes borylated products in moderate to excellent yields. We proposed the formation of the EDA complex between thiolate/B<sub>2</sub>pin<sub>2</sub> and boryl-anion-activated substrate as the key step to obtain the reactivity, which is supported by UV-vis measurements, NMR analysis and control experiments. This combination of photochemistry with thiolate catalysis constitutes a unique activation mode of substituted arenes in cross-coupling reactions. Further studies regarding elucidation the detailed reaction mechanism and the extension of this catalytic system to other coupling partners are currently underway in our laboratory.

## Acknowledgements

This project has received funding from the European Research Council (ERC) under the European Unions Horizon 2020 research and innovation programme (grant agreement No. 741623). S.W. thanks the China Scholarship Council (CSC) for a predoctoral fellowship (CSC student number 201606280052). We are grateful to Prof. Armido Studer (University of Münster) for helpful discussions. We further thank Dr. Rudolf Vasold (University of Regensburg) for his assistance in GC-MS measurements and Ms. Regina Hoheisel (University of Regensburg) for her assistance in cyclic voltammetry measurements.

## Author Contributions

B.K. supervised the project. S.W. developed the catalytic system, conducted the experiments and analyzed the data; S.W. and H.W. conducted the mechanistic studies; S.W. and B.K. wrote the manuscript with input from all of the authors.

## Notes

The authors declare no competing financial interests.

## Reference

1. Narayanam, J. M. R., Stephenson, C. R. J. (2011). Visible light photoredox catalysis: applications in organic synthesis. *Chem. Soc. Rev.* *40*, 102-113.
2. Xuan, J., Xiao, W.-J. (2012). Visible-Light Photoredox Catalysis. *Angew. Chem. Int. Ed.* *51*, 6828-6838.
3. Prier, C. K., Rankic, D. A., MacMillan, D. W. C. (2013). Visible Light Photoredox Catalysis with Transition Metal Complexes: Applications in Organic Synthesis. *Chem. Rev.* *113*, 5322-5363.
4. Romero, N. A., Nicewicz, D. A. (2013). Organic Photoredox Catalysis. *Chem. Rev.* *116*, 10075-10166.
5. Skubi, K. L., Blum, T. R., Yoon, T. P. (2013). Dual Catalysis Strategies in Photochemical Synthesis. *Chem. Rev.* *116*, 10035-10074.
6. Marzo, L., Pagire, S. K., Reiser, O., König, B. (2013). Visible-Light Photocatalysis: Does It Make a Difference in Organic Synthesis? *Angew. Chem. Int. Ed.* *57*, 10034-10072.
7. Glaser, F., Kerzig, C., Wenger, O. S. (2013). Multi-Photon Excitation in Photoredox Catalysis: Concepts, Applications, Methods. *Angew. Chem. Int. Ed.* *59*, 10266-10284.
8. Ghosh, I., Marzo, L., Das, A., Shaikh, R., König, B. (2013). Visible Light Mediated Photoredox Catalytic Arylation Reactions. *Acc. Chem. Res.* *49*, 1566-1577.
9. Majek, M., Jacobi von Wangelin, A. (2016). Mechanistic Perspectives on Organic Photoredox Catalysis for Aromatic Substitutions. *Acc. Chem. Res.* *49*, 2316-2327.
10. Ghosh, I. (2019). Excited radical anions and excited anions in visible light photoredox catalysis.

Phys. Sci. Rev. 4, 20170185.

11. Ghosh, I., Ghosh, T., Bardagi, J. I., König, B. (2014). Reduction of aryl halides by consecutive visible light-induced electron transfer processes. *Science* 346, 725-728.
12. Giedyk, M., Narobe, R., Weiß, S., Touraud, D., Kunz, W., König, B. (2020). Photocatalytic activation of alkyl chlorides by assembly-promoted single electron transfer in microheterogeneous solutions. *Nat. Catal.* 3, 40-47.
13. Ghosh, I., König, B. (2016). Chromoselective Photocatalysis: Controlled Bond Activation through Light-Color Regulation of Redox Potentials. *Angew. Chem. Int. Ed.* 55, 7676-7679.
14. Cowper, N. G. W., Chernowsky, C. P., Williams, O. P., Wickens, Z. K. (2020). Potent Reductants via Electron-Primed Photoredox Catalysis: Unlocking Aryl Chlorides for Radical Coupling. *J. Am. Chem. Soc.* 142, 2093-2099.
15. Kim, H., Kim, H., Lambert, T. H., Lin, S. (2020). Reductive Electrophotocatalysis: Merging Electricity and Light To Achieve Extreme Reduction Potentials. *J. Am. Chem. Soc.* 142, 2087-2092.
16. MacKenzie, I. A., Wang, L., Onuska, N. P. R., Williams, O. F., Begam, K., Moran, A. M., Dunietz, B. D., Nicewicz, D. A. (2020). Discovery and characterization of an acridine radical photoreductant. *Nature* 580, 76-80.
17. Schmalzbauer, M., Marcon, M., König, B. (2020). Excited State Anions in Organic Transformations. *Angew. Chem. Int. Ed.* 10.1002/anie.202009288.
18. Boronic Acids: Preparation and Applications in Organic Synthesis, Medicine and Materials, 2nd ed., Hall, D. G., Ed., Wiley-VCH: Weinheim, Germany, 2011
19. Miyaura, N., Suzuki, A. (1995). Palladium-Catalyzed Cross-Coupling Reactions of Organoboron Compounds. *Chem. Rev.* 95, 2457-2483.
20. Ishiyama, T., Murata, M., Miyaura, N. (1995), Palladium(0)-Catalyzed Cross-Coupling Reaction of Alkoxydiboron with Haloarenes: A Direct Procedure for Arylboronic Esters. *J. Org. Chem.* 60, 7508-7510.
21. Neeve, E. C., Geier, S. J., Mkhaliid, I. A. I., Westcott, S. A., Marder, T. B. (2016). Diboron(4) Compounds: From Structural Curiosity to Synthetic Workhorse. *Chem. Rev.* 116, 9091-9161.
22. Friese, F. W., Studer, A. (2019). New avenues for C–B bond formation via radical intermediates. *Chem. Sci.* 10, 8503-8518.
23. Nguyen, V. D., Nguyen, V. T., Jin, S., Dang, H. T., Larionov, O. V. (2019). Organoboron chemistry comes to light: Recent advances in photoinduced synthetic approaches to organoboron compounds. *Tetrahedron.* 75, 584-602.
24. Wang, M., Shi, Z. (2019). Methodologies and Strategies for Selective Borylation of C–Het and C–C Bonds. *Chem. Rev.* 120, 7348-7398.
25. Yan, G., Huang, D., Wu, X. (2018). Recent Advances in C–B Bond Formation through a Free Radical Pathway. *Adv. Synth. Catal.* 360, 1040-1053.
26. Yu, J., Zhang, L., Yan, G. (2012). Metal-Free, Visible Light-Induced Borylation of Aryldiazonium Salts: A Simple and Green Synthetic Route to Arylboronates. *Adv. Synth. Catal.* 354, 2625-2628.
27. Ahammed, S., Nandi, S., Kundu, D., Ranu, B. C. (2016). One-pot Suzuki coupling of aromatic amines via visible light photocatalyzed metal free borylation using t-BuONO at room temperature. *Tetrahedron Lett.* 57, 1551-1554.
28. Lei, T., Wei, S.-M., Feng, K., Chen, B., Tung, C.-H., Wu, L.-Z. (2020). Borylation of Diazonium Salts by Highly Emissive and Crystalline Carbon Dots in Water. *ChemSusChem.* 13, 1715-1719.

29. Mfuh, A. M., Doyle, J. D., Chhetri, B., Arman, H. D., Larionov, O. V. (2016). Scalable, Metal- and Additive-Free, Photoinduced Borylation of Haloarenes and Quaternary Arylammonium Salts. *J. Am. Chem. Soc.* *138*, 2985-2988.
30. Jin, S., Dang, H. T., Haug, G. C., He, R., Nguyen, V. D., Nguyen, V. T., Arman, H. D., Schanze, K. S., Larionov, O. V. (2020). Visible Light-Induced Borylation of C–O, C–N, and C–X Bonds. *J. Am. Chem. Soc.* *142*, 1603-1613.
31. Chen, K., Zhang, S., He, P., Li, P. (2016). Efficient metal-free photochemical borylation of aryl halides under batch and continuous-flow conditions. *Chem. Sci.* *7*, 3676-3680.
32. Jiang, M., Yang, H., Fu, H. (2016). Visible-Light Photoredox Borylation of Aryl Halides and Subsequent Aerobic Oxidative Hydroxylation. *Org. Lett.* *18*, 5248-5251.
33. Cheng, Y., Mück-Lichtenfeld, C., Studer, A. (2018). Metal-Free Radical Borylation of Alkyl and Aryl Iodides. *Angew. Chem. Int. Ed.* *57*, 16832-16836.
34. Qiao, Y., Yang, Q., Schelter, E. J. (2018). Photoinduced Miyaura Borylation by a Rare-Earth-Metal Photoreductant: The Hexachloroacetate(III) Anion. *Angew. Chem. Int. Ed.* *57*, 10999-11003.
35. Zhang, L., Jiao, L. (2019). Visible-Light-Induced Organocatalytic Borylation of Aryl Chlorides. *J. Am. Chem. Soc.* *141*, 9124-9128.
36. Tian, Y.-M., Guo, X.-N., Krummenacher, I., Wu, Z., Nitsch, J., Braunschweig, H., Radius, U., Marder, T. B. (2020). Visible-Light-Induced Ni-Catalyzed Radical Borylation of Chloroarenes. *J. Am. Chem. Soc.* *142*, 18231-18242.
37. Tian, Y.-M., Guo, X.-N., Kuntze-Fechner, M. W., Krummenacher, I., Braunschweig, H., Radius, U., Steffen, A., Marder, T. B. (2018). Selective Photocatalytic C–F Borylation of Polyfluoroarenes by Rh/Ni Dual Catalysis Providing Valuable Fluorinated Arylboronate Esters. *J. Am. Chem. Soc.* *140*, 17612-17623.
38. Liu, W., Yang, X., Gao, Y., Li, C.-J. (2017). Simple and Efficient Generation of Aryl Radicals from Aryl Triflates: Synthesis of Aryl Boronates and Aryl Iodides at Room Temperature. *J. Am. Chem. Soc.* *139*, 8621-8627.
39. Nitelet, A., Thevenet, D., Schiavi, B., Hardouin, C., Fournier, J., Tamion, R., Pannecoucke, X., Jubault, P., Poisson, T. (2019). Copper-Photocatalyzed Borylation of Organic Halides under Batch and Continuous-Flow Conditions. *Chem. Eur. J.* *25*, 3262-3266.
40. Candish, L., Teders, M., Glorius, F. (2017). Transition-Metal-Free, Visible-Light-Enabled Decarboxylative Borylation of Aryl N-Hydroxyphthalimide Esters. *J. Am. Chem. Soc.* *139*, 7440-7443.
41. Schmalzbauer, M., Svejstrup, T. D., Fricke, F., Brandt, P., Johansson, M. J., Bergonzini, G., König, B. (2020). Redox-Neutral Photocatalytic C–H Carboxylation of Arenes and Styrenes with CO<sub>2</sub>. *Chem* *6*, 2658 - 2672.
42. Schmalzbauer, M., Ghosh, I., König, B. (2019). Utilising excited state organic anions for photoredox catalysis: activation of (hetero)aryl chlorides by visible light-absorbing 9-anthrolate anions. *Faraday Discuss.* *215*, 364-378.
43. Wang, S., Lokesh, N., Hioe, J., Gschwind, R. M., König, B. (2019). Photoinitiated carbonyl-metathesis: deoxygenative reductive olefination of aromatic aldehydes via photoredox catalysis. *Chem. Sci.* *10*, 4580-4587.
44. Liu, B., Lim, C.-H., Miyake, G. M. (2017). Visible-Light-Promoted C–S Cross-Coupling via Intermolecular Charge Transfer. *J. Am. Chem. Soc.* *139*, 13616-13619.
45. de Pedro Beato, E., Mazzarella, D., Balletti, M., Melchiorre, P. (2020). Photochemical generation of acyl and carbamoyl radicals using a nucleophilic organic catalyst: applications and

mechanism thereof. *Chem. Sci.* *11*, 6312-6324.

46. Mazzarella, D., Magagnano, G., Schweitzer-Chaput, B., Melchiorre, P. (2019). Photochemical Organocatalytic Borylation of Alkyl Chlorides, Bromides, and Sulfonates. *ACS Catal.* *9*, 5876-5880.
47. Schweitzer-Chaput, B., Horwitz, M. A., de Pedro Beato, E., Melchiorre, P. (2019). Photochemical generation of radicals from alkyl electrophiles using a nucleophilic organic catalyst. *Nat. Chem.* *11*, 129-135.
48. Spinnato, D., Schweitzer-Chaput, B., Goti, G., Ošek, M., Melchiorre, P. (2020). A Photochemical Organocatalytic Strategy for the  $\alpha$ -Alkylation of Ketones by using Radicals. *Angew. Chem. Int. Ed.* *59*, 9485-9490.
49. Huang, H., Ye, J.-H., Zhu, L., Ran, C.-K., Miao, M., Wang, W., Chen, H., Zhou, W.-J., Lan, Y., Yu, B., Yu, D.-G. (2020). Visible-Light-Driven Anti-Markovnikov Hydrocarboxylation of Acrylates and Styrenes with CO<sub>2</sub>. *CCS Chem.* *2*, 1746-1756.
50. During the preparation of this manuscript, Chiba and co-workers reported a polysulfide anion catalysis for the generation of aryl radicals from arene halides under light irradiation. However, the reaction could only be employed for the reduction of activated substrates. See: Li, H. Y., Tang, X. X., Pang, J. H., Wu, X. Y., Yeow, Edwin K. L., Wu, J., Shunsuke, C. (2020). Polysulfide Anions as Visible Light Photoredox Catalysts for Aryl Cross-Couplings. *ChemRxiv*. Preprint. <https://doi.org/10.26434/chemrxiv.13083887.v1>.
51. Chen, K., Cheung, M. S., Lin, Z., Li, P. (2016). Metal-free borylation of electron-rich aryl (pseudo)halides under continuous-flow photolytic conditions. *Org. Chem. Front.* *3*, 875-879.
52. Zeng, H., Qiu, Z., Domínguez-Huerta, A., Hearne, Z., Chen, Z., Li, C.-J. (2017). An Adventure in Sustainable Cross-Coupling of Phenols and Derivatives via Carbon–Oxygen Bond Cleavage. *ACS Catal.* *7*, 510-519.
53. Qiu, Z., Li, C.-J. (2020). Transformations of Less-Activated Phenols and Phenol Derivatives via C–O Cleavage. *Chem. Rev.* *120*, 10454-10515.
54. Kaiser, D., Klose, I., Oost, R., Neuhaus, J., Maulide, N. (2019). Bond-Forming and -Breaking Reactions at Sulfur(IV): Sulfoxides, Sulfonium Salts, Sulfur Ylides, and Sulfinate Salts. *Chem. Rev.* *119*, 8701-8780.
55. Gao, J., Feng, J., Du, D. (2020). Shining Light on C–S Bonds: Recent Advances in C–C Bond Formation Reactions via C–S Bond Cleavage under Photoredox Catalysis. *Chem. Asian J.* *15*, 3637–3659.
56. Huang, C., Feng, J., Ma, R., Fang, S., Lu, T., Tang, W., Du, D., Gao, J. (2019). Redox-Neutral Borylation of Aryl Sulfonium Salts via C–S Activation Enabled by Light. *Org. Lett.* *21*, 9688-9692.
57. Maekawa, Y., Ariki, Z. T., Nambo, M., Crudden, C. M. (2019). Pyridine-catalyzed desulfonative borylation of benzyl sulfones. *Org. Biomol. Chem.* *17*, 7300-7303.
58. Raviola, C., Protti, S. (2019). Leaving Groups in Metal-Free Arylations: Make Your Choice! *Eur. J. Org. Chem.* *2020*, 5292-5304.
59. Crisenza, G. E. M., Mazzarella, D., Melchiorre, P. (2020). Synthetic Methods Driven by the Photoactivity of Electron Donor–Acceptor Complexes. *J. Am. Chem. Soc.* *142*, 5461-5476.
60. Lima, C. G. S., de M. Lima, T., Duarte, M., Jurberg, I. D., Paixão, M. W. (2016). Organic Synthesis Enabled by Light-Irradiation of EDA Complexes: Theoretical Background and Synthetic Applications. *ACS Catal.* *6*, 1389-1407.
61. Cheng, W.-M., Shang, R., Zhao, B., Xing, W.-L., Fu, Y. (2017). Isonicotinate Ester Catalyzed

Decarboxylative Borylation of (Hetero)Aryl and Alkenyl Carboxylic Acids through N-Hydroxyphthalimide Esters. *Org. Lett.* *19*, 4291-4294.

62. Nguyen, P., Dai, C., Taylor, N. J., Power, W. P., Marder, T. B., Pickett, N. L., Norman, N. C. (1995). Lewis Base Adducts of Diboron Compounds: Molecular Structures of [B<sub>2</sub>(cat)<sub>2</sub>(4-picoline)] and [B<sub>2</sub>(cat)<sub>2</sub>(4-picoline)<sub>2</sub>] (cat = 1,2-O<sub>2</sub>C<sub>6</sub>H<sub>4</sub>). *Inorg. Chem.* *34*, 4290-4291.

63. Katsuma, Y., Asakawa, H., Yamashita, M. (2018). Reactivity of highly Lewis acidic diborane(4) towards pyridine and isocyanide: formation of boraalkene-pyridine complex and ortho-functionalized pyridine derivatives. *Chem. Sci.* *9*, 1301-1310.

64. Pietsch, S., Neeve, E. C., Apperley, D. C., Bertermann, R., Mo, F., Qiu, D., Cheung, M. S., Dang, L., Wang, J., Radius, U., Lin, Z., Kleeberg, C., Marder, T. B. (2015). Synthesis, Structure, and Reactivity of Anionic sp<sup>2</sup>-sp<sup>3</sup> Diboron Compounds: Readily Accessible Boryl Nucleophiles. *Chem. Eur. J.* *21*, 7082-7098.

65. Pinet, S., Liautard, V., Debais, M., Pucheault, M. (2017). Radical metal-free borylation of aryl iodides. *Synthesis* *49*, 4759-4768.

66. Lu, J., Khetrapal, N. S., Johnson, J. A., Zeng, X. C., Zhang, J. (2016). "π-Hole-π" Interaction Promoted Photocatalytic Hydrodefluorination via Inner-Sphere Electron Transfer. *J. Am. Chem. Soc.* *138*, 15805-15808.

